

Modulated Morphology in the Self-Organization of a Rectangular Amphiphile

Fátima García, Gustavo Fernández, and Luis Sánchez*^[a]

Abstract: The rectangular oligo(phenylene ethynylene) amphiphile **1** has been synthesized to investigate its self-assembling features in solution and onto surfaces. Concentration-dependent and variable-temperature NMR experiments firstly demonstrate the influence of the solvent in the stabilization of the non-covalent forces involved in the association of **1**, namely, π - π stacking interactions between the aromatic fragments and van der Waals, hydrogen-bonding and/or solvophobic forces between the triethyleneglycol chains. This subtle balance of non-co-

valent interactions also conditions the thermodynamics of the self-assembly process and concentration-dependent UV/Vis investigations show a linear correlation between the polarity of the solvent and the K_a values ($K_a \approx 5.2 \times 10^5 \text{ M}^{-1}$ for $\text{CH}_3\text{CN}/\text{H}_2\text{O}$ mixtures and $4.4 \times 10^4 \text{ M}^{-1}$ for benzene). Moreover, these UV/Vis studies prove the organization of this compound following the

Keywords: amphiphiles • micelles • supramolecular chemistry • toroids • vesicles

indefinite self-association model. Microscopy techniques reveal that the morphology and dimensionality of the assemblies formed from **1** can be finely modulated. Although polar solvents yield hollow vesicles or toroidal 3D objects, depending upon concentration, the utilization of non-polar benzene results in the formation of unimolecular wires that can grow to form networks upon increasing concentration. These findings support the direct relationship existing between the self-assembling features of this amphiphile in solution and onto surfaces.

Introduction

Amphiphilic systems, that is, those systems that bear hydrophilic and hydrophobic fragments in a determined proportion, are ubiquitous in living organisms and have found application in industrial and domestic utilities.^[1] The spontaneous self-assembly that these compounds achieve, a consequence of the synergy of a number of weak forces in a delicate balance, can be finely tuned by subtle modifications in the chemical structure or in the external conditions like concentration, temperature, time, etc. These modifications can generate supramolecular arrays of different morphology and/or dimensionality.^[2] A direct effect of this “soft-matter polymorphism”^[3] is the change in the dimensionality and the morphology of the supramolecular ensembles, and also in their physico-chemical properties and applications.^[4]

Small block molecules in which the relative proportion between a rigid aromatic and hydrophobic core and its surrounding flexible coils, which can behave as hydrophobic or hydrophilic units, are outstanding examples of artificial amphiphilic systems capable to self-organize into a variety of well-ordered non-covalent architectures.^[5] Modifications in the number, the length or the shape of the aromatic units and/or in the length or nature (linear or branched) of the oligoether hydrophilic chains change the subtle balance of the different non-covalent interactions between the hydrophobic and hydrophilic groups and induce the self-aggregation of small amphiphilic molecules into organized non-covalent architectures like micelles,^[6] fibres,^[7] or vesicles.^[8] Very recently, we have reported on the solvent-controlled self-assembly of a C_3 -symmetric radial oligo(phenylene ethynylene) (OPE) amphiphile. This amphiphile self-assembles into vesicles, networks or rods depending on the nature of the solvent used. Whereas the use of polar solvents induces the rearrangement of the amphiphile into hollow vesicles, in moderate-to-low polarity solvents the dimensionality of the objects formed in solution and on solid substrates decreases gradually upon decreasing solvent polarity.^[9]

The creation of the above mentioned superstructures is dominated by π - π interactions of the aromatic backbone

[a] F. García, Dr. G. Fernández, Dr. L. Sánchez
Departamento de Química Orgánica
Facultad de Ciencias Químicas
Ciudad Universitaria s/n. 28040 Madrid (Spain)
Fax: (+34) 913944103
E-mail: lusamar@quim.ucm.es

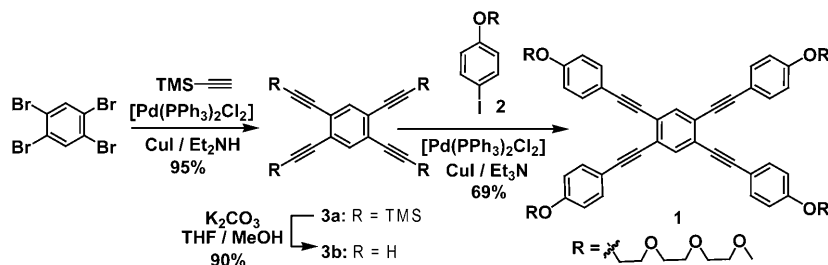
 Supporting information for this article is available on the WWW under <http://dx.doi.org/10.1002/chem.200900303>.

surrounded by a variable number of hydrophilic chains. Nevertheless, π - π interactions—considered as the sum of several non-covalent forces like electrostatic, attractive and repulsive orbital interactions and solvophobic effects^[10]—are not the only supramolecular forces participating in the self-assembly and some other non-covalent forces cooperate and play a crucial role in the formation of the supramolecular ensembles.^[11] The self-assembly of small amphiphilic molecules is, therefore, a useful benchmark to understand and quantify all these non-covalent forces that finally control the creation of structures with variable morphologies.

Herein, we report on the synthesis and self-assembling features of a simple rectangular OPE amphiphile **1** in which a central aromatic core is surrounded by four hydrophilic triethyleneglycol (TEG) chains. Based on our previous results on radial amphiphilic OPEs, we now set up to investigate how subtle changes in the chemical structure and, in consequence, in the hydrophylic/hydrophobic ratio of this class of amphiphiles strongly influence their self-assembly process and, hence, the final morphology of the aggregates.

Results and Discussion

Synthesis: Rectangular-shaped amphiphile **1** was straightforwardly obtained in only four synthetic steps and its synthesis is depicted in Scheme 1. The peripheral hydrophilic aromat-



Scheme 1. Synthesis of the rectangular amphiphilic OPE **1**.

ic units (**2**) were prepared by following a Mitsunobu's protocol^[12] as previously reported.^[9] The synthesis of the central aromatic moiety (**3a**)^[13] was achieved by using a Sonogashira cross-coupling reaction^[14] between 1,2,4,5-tetrabromobenzene and (trimethylsilyl)-acetylene (TMS) and subsequent deprotection with K_2CO_3 . A final Sonogashira cross-coupling reaction between **2** and **3b**^[13] affords compound **1** in 69% yield. Compound **1** has been fully characterized by using NMR, FTIR and UV/Vis spectroscopy and MALDI-TOF spectrometry (see the Supporting Information).

MALDI-TOF spectrometry not only provides structural information, but is also a powerful tool to investigate the capability of organic substances to interact supramolecularly.^[15] For the case of compound **1**, besides the molecular peak at m/z 1126 (Figure S1 in the Supporting Information), signals corresponding to the dimer (m/z 2252) and trimer

(m/z 3378) are clearly noticeable (Figure 1). This observation provided a first insight into the strong tendency of **1** to self-assemble by means of π - π interactions and especially, by the influence of the solvophobic component.^[16]

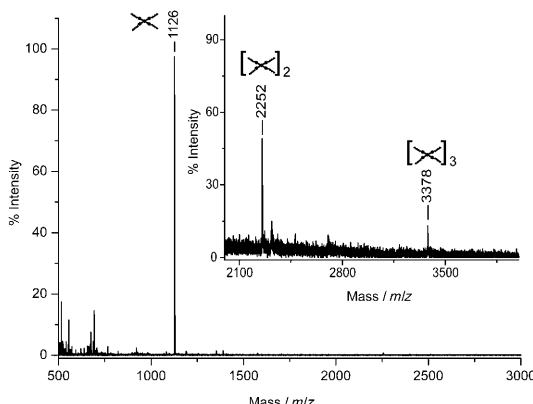


Figure 1. MALDI-TOF (ditranol) mass spectrum of amphiphile **1**. The inset shows the formation of aggregates in the gas phase.

Self-assembly in solution: The self-assembly of **1** in solution has been investigated by using concentration-dependent and variable-temperature (VT) 1H NMR experiments as well as concentration-dependent UV/Vis investigations in different solvents. The 1H NMR spectra of **1** in CD_3CN (300 MHz, 298 K) at concentrations between 1.5 and 100 mM is shown in Figure S2 in the Supporting Information. As the concentration increases, a slight shielding of most resonances is observed, which indicates the formation of aggregates of **1**. This shift pattern, in which all the resonances are affected upon increasing concentration, clearly indicates that the radial OPE

systems are arranged in an eclipsed fashion. The self-assembly process is induced by a face-to-face π -stacking of the aromatic units reinforced by the van der Waals contacts between the peripheral TEG chains.^[9] To further investigate the role that the stacking aromatic interactions and other non-covalent forces play in the self-assembly of amphiphile **1**, we also performed VT 1H NMR experiments in deuterated acetonitrile (Figure 2). A clear broadening and slight shielding of most resonances, especially the TEG chains, is observed upon decreasing temperature. A detailed analysis of the concentration and temperature dependence of the chemical shifts shows a linear behaviour, although with different slope values for the aromatic (\bullet) or aliphatic (\blacklozenge) resonances (Figure 2b,c). The dissimilar effect of the concentration and temperature on the δ value for these signals could be attributable to the different nature and participation

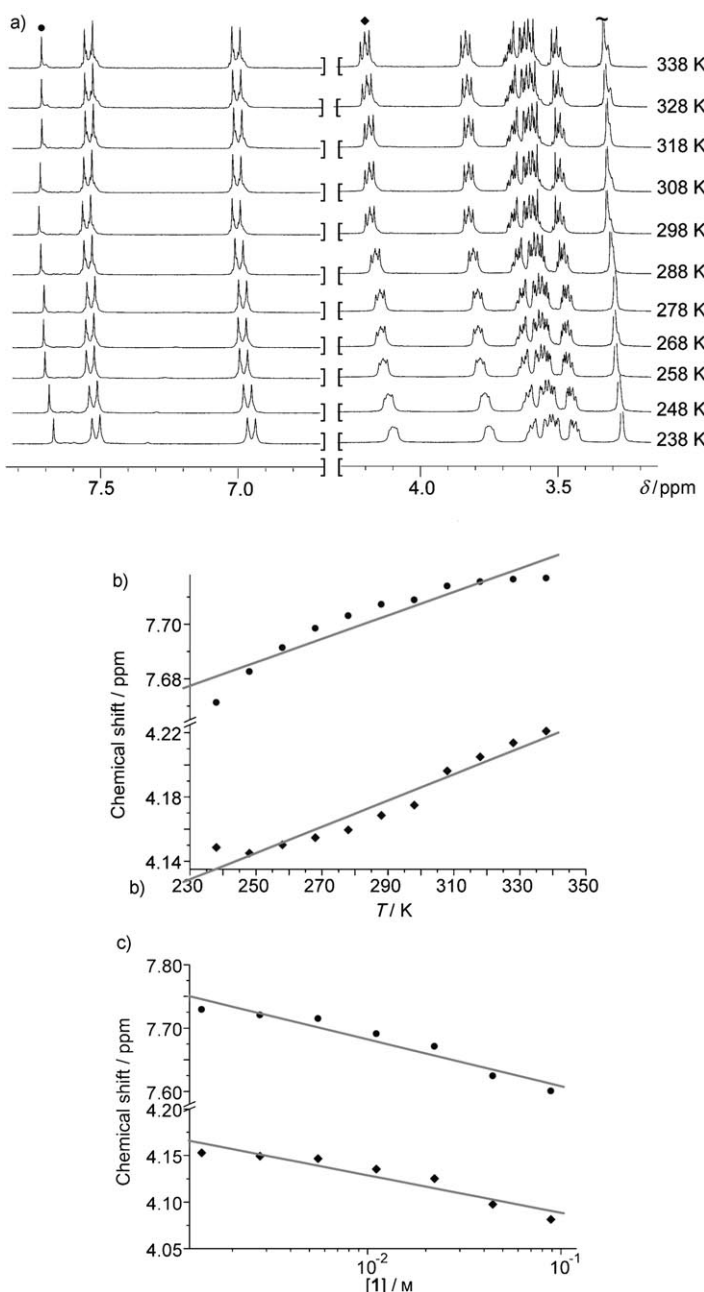


Figure 2. a) Partial ^1H NMR spectra (CD_3CN , 300 MHz, 4 mM) of **1** at different temperatures. Linear relationship of chemical shifts corresponding to the proton at $\delta \approx 7.7$ and ≈ 4.1 ppm against b) temperature (\bullet , slope = 7.5, $R = -0.94$; \blacklozenge , slope = 3.8, $R = 0.96$) and c) concentration (\bullet , slope = 7.5, $R = -0.96$; \blacklozenge , slope = 4.0, $R = -0.94$).

degree of the non-covalent forces involved in the interaction of the aromatic fragments or the TEG chains. Although $\pi-\pi$ interactions between the aromatic central core of **1** dominate its self-assembly, other supramolecular forces (solvophobic, H-bonding) coming from the TEG chains contribute in a lesser extent.^[11a, 17–19]

Decreasing the polarity of the solvent should induce the coiling of the TEG chains and the association of **1** in a rotated fashion.^[9] Concentration-dependent ^1H NMR experi-

ments carried out in deuterated benzene (Figure S3) show little changes in all resonances. As the concentration increases, the proton corresponding to the central aromatic ring experiences a slight upfield shift whereas only one of the peripheral *para*-substituted aromatic protons shifts downfield. VT ^1H NMR studies confirm this tendency, which suggests the mentioned rotated aggregation of molecules of **1** to form a columnar stack. Similarly to the analysis carried out in CD_3CN , the concentration and temperature dependence of the chemical shifts in C_6D_6 corroborates a linear behaviour with a steeper slope for the aromatic protons than that for the aliphatic ones (Figure S3).

The slight shifts observed in the NMR studies and the linear behaviour observed for the concentration and temperature variation of the chemical shifts could be indicative of a high value for the binding constant (K_a). Thus, an accurate calculation of this thermodynamical parameter by using this technique would need highly diluted concentrations not detectable in the NMR time-scale. To determine a precise value for K_a , we carried out concentration-dependent UV/Vis studies utilizing CH_3CN as solvent. The UV/Vis spectra of **1** in CH_3CN (298 K) at different concentrations is shown in Figure S4. As the concentration increases the depletion of the absorption band at $\lambda \approx 280$ nm is accompanied by the emergence of two new broad transitions that spread into the visible region up to $\lambda \approx 400$ nm (Figure S4b). The first band is assigned to small or free species of **1**, whereas the two less energetic waves correspond to larger supramolecular aggregates resulting from the $\pi-\pi$ interactions between the aromatic units of **1**. The spectroscopic changes observed in the concentration-dependent UV/Vis experiments were fitted to the isodesmic model^[20] applied to the molar extinction coefficient^[9,21] at a wavelength of 328 nm affording large K_a values ($\approx 3.8 \times 10^5 \text{ M}^{-1}$), which demonstrates the great ability of **1** to self-assemble in polar solvents. The effect exerted by water molecules on the self-assembly of **1** has been also investigated by concentration-dependent UV/Vis experiments in $\text{CH}_3\text{CN}/\text{H}_2\text{O}$ (1:1) mixtures (Figure 3a). These studies show similar spectra than those registered in pure CH_3CN with an identical pattern of absorption bands. However, in this case, a K_a value of $5.2 \times 10^5 \text{ M}^{-1}$, practically twice the value observed in CH_3CN , was calculated.

The larger K_a value determined for the more polar $\text{CH}_3\text{CN}/\text{H}_2\text{O}$ mixture reveals the importance of water in the stabilization of some of the non-covalent forces involved in the self-assembly of **1**, namely, the interactions between polar TEG chains,^[5] and the solvophobic interactions between the aromatic fragments. In these conditions, water molecules can choose between a weak interaction with the aromatic and nonpolar OPE backbone of **1** and a much more energetically favourable interaction with another solvent molecule. Highly polar solvents are predisposed to form a cage around nonpolar solutes, like hydrocarbons, to minimize solvent-solute interactions.^[10] This positive solute-solute solvophobic interaction among OPE fragments of adjacent molecules of **1** strengthens the global π -stacking of the aromatic rings and increases the K_a values. Furthermore,

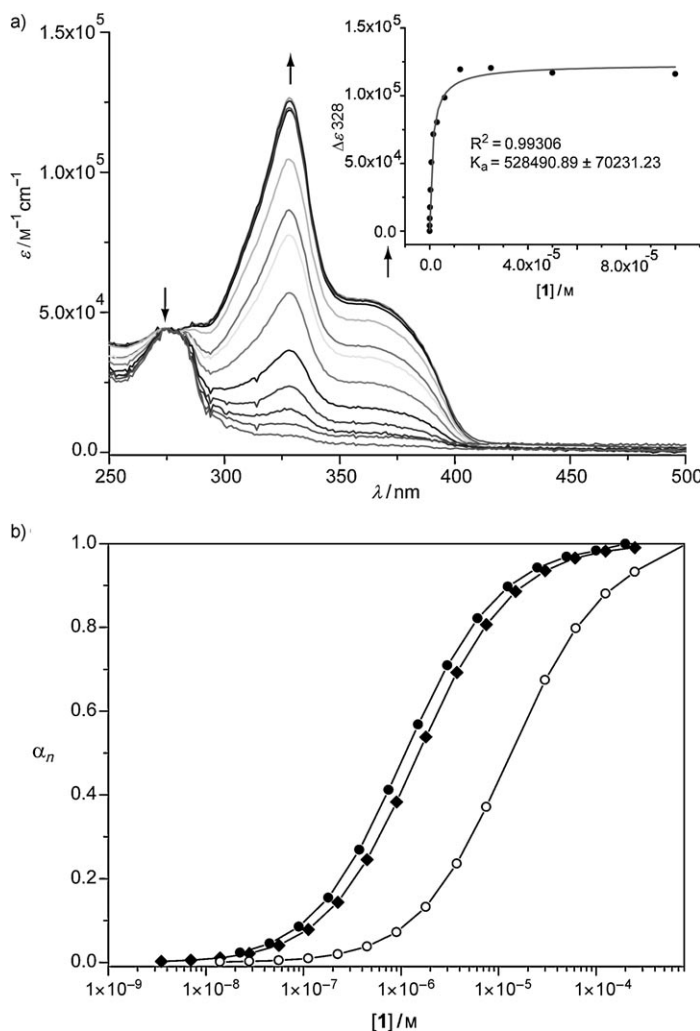


Figure 3. a) Normalized UV/Vis absorption spectra of **1** ($\text{CH}_3\text{CN}/\text{H}_2\text{O}$, 1:1, 298 K, 2.5×10^{-4} to 4.5×10^{-8} M). Arrows indicate the direction of change with increasing concentration. The inset in (a) shows the fit of $\Delta\epsilon$ (328 nm) to the isodesmic model;^[9,21] b) molar fraction of aggregates (α_n) of **1** as a function of concentration in different solvents; $\text{H}_2\text{O}/\text{MeCN}$ (●), MeCN (◆), C_6H_6 (○).^[22]

polar solvent molecules act as cement inducing the attractive interaction between the hydrophilic TEG chains. The significance of the solvent in the thermodynamics of the self-assembly of **1** has been further corroborated by using non-polar benzene. The corresponding concentration-dependent UV/Vis studies show a similar pattern for the absorption bands than the observed in the studies developed in MeCN or $\text{H}_2\text{O}/\text{MeCN}$ mixtures but a K_a value of $4.4 \times 10^4 \text{ M}^{-1}$, an order of magnitude lower than the value calculated for polar solvents, was obtained (Figure S5). The decreasing trend observed for K_a with decreasing the polarity of the solvent demonstrates the relevance of solvophobic interactions in the association of amphiphile **1**.^[10]

The validity of the isodesmic model for the self-assembly of **1** has been further corroborated by the determination of the molar fraction of *n*-mer aggregates (α_n) in the experimental conditions of concentration and solvents (Fig-

ure 3 b).^[20–22] The α_n value, together with the K_a , is indicative of the propensity of the system to form supramolecular stacks. As expected, the increase of α_n , and therefore the self-aggregation process, starts at lower concentrations for the more polar $\text{H}_2\text{O}/\text{MeCN}$ mixtures than in MeCN or benzene. A similar trend is observed for the average amphiphile number per stack (N) (Figure S6).^[20–22]

The association studies of **1** in solution have been complemented by dynamic light scattering (DLS) measurements (Figure 4). This technique allows an accurate determination

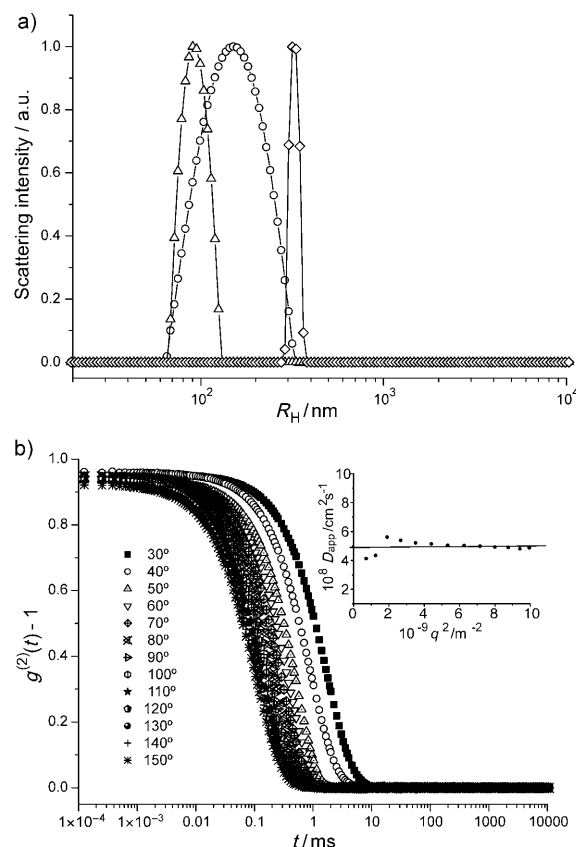


Figure 4. a) Distribution of hydrodynamic radii of aggregates of **1** in different solvents; MeCN, 10^{-4} M (Δ); $\text{H}_2\text{O}/\text{MeCN}$, 10^{-4} M (\diamond); $\text{H}_2\text{O}/\text{MeCN}$, 10^{-6} M (\circ). b) Autocorrelation functions for a $\approx 10^{-4}$ M solution of **1** in acetonitrile/ H_2O (1:1). The inset shows the angular dependence of apparent diffusion coefficient versus the angle q .

of the particle size and shape. Narrow distributions of aggregates with calculated hydrodynamic radii (R_H) of around 100 and 200 nm were observed for $\approx 10^{-4}$ M solutions of **1** in CH_3CN and 1/1 $\text{CH}_3\text{CN}/\text{H}_2\text{O}$ mixtures, respectively. For the latter case, CONTIN analysis of the DLS autocorrelation functions (Figure 3b) demonstrates the lack of angular dependence for the apparent diffusion coefficient (D_{app}) (inset in Figure 4b), which could be indicative of the formation of spherical objects.^[6a,23]

The DLS analysis for a $\approx 10^{-6}$ M solution of **1** in $\text{CH}_3\text{CN}/\text{H}_2\text{O}$ (1:1) mixtures showed, unexpectedly, a broad distribution for the aggregates centred at a R_H value of around

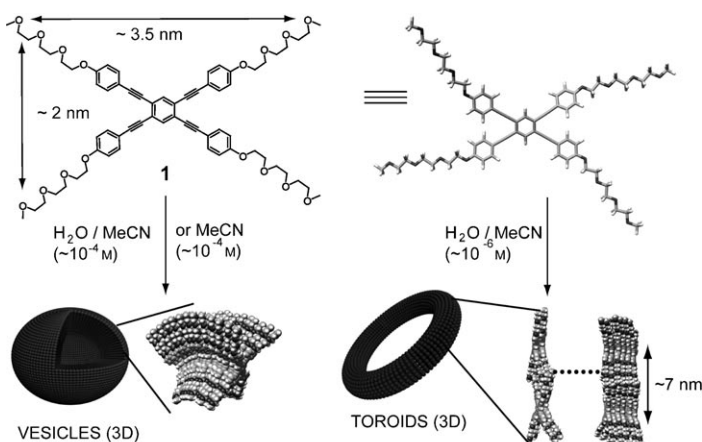
150 nm, a size larger than that calculated for more concentrated conditions (Figure 4a). This broad distribution could imply the presence of species of different morphology.^[24] On the other hand, using non-polar benzene to determine the R_H value in benzene only resulted in the apparition of broad and variable contributions that indicates the presence of fluctuating species whose size and/or shape changes rapidly.

Self-assembly onto surfaces: All the above studies, carried out in solution, demonstrate the presence of aggregated species that could be effectively transferred onto a substrate. The morphology and dimensionality of these aggregates has been examined by atomic force microscopy (AFM) utilizing different experimental conditions (Scheme 2). Thus, AFM images of $\approx 10^{-4}$ M solutions of **1** in polar solvents (CH_3CN or $\text{CH}_3\text{CN}/\text{H}_2\text{O}$ mixtures) drop-cast onto mica displayed flattened spherical vesicles (Figure S8 and Figure 5). In good agreement with DLS measurements, the vesicles show mean diameters of 80 ± 10 nm and heights of 12 ± 2 nm for the $\approx 10^{-4}$ M solution of **1** in CH_3CN , being the average dia-

ters and heights of 220 ± 13 and 25 ± 1 nm, respectively, for the $\text{CH}_3\text{CN}/\text{H}_2\text{O}$ mixtures (Figure 4a).^[25]

Fluorescence microscopy images of **1** in these conditions provide first evidence on the hollow nature of the vesicles (Figure S9). In this case, hollow circular objects with an average diameter of ≈ 200 nm were observed, in a very good agreement with the previous AFM images. In addition, TEM images registered from $\approx 10^{-4}$ M $\text{CH}_3\text{CN}/\text{H}_2\text{O}$ mixtures of **1** onto carbon-coated grids and negatively stained with uranyl acetate, confirm the formation of hollow vesicles with diameters in the range of 200 nm (Figure 5b). The formation of unimolecular π -stacked curved segments of **1** between the aromatic moieties and the van der Waals contacts between the TEG chains could account for the mechanism of vesicle formation (Scheme 2 and Figure S1). At this relatively high content of amphiphilic molecules, hollow spherical objects guarantee the maximal area of exposure for the hydrophilic TEG chains to interact with polar solvents.

To clarify the unexpected increasing in size of the aggregates upon decreasing concentration observed in DLS experiments, we also performed AFM experiments from a solution of **1** ($\approx 10^{-6}$ M) in $\text{H}_2\text{O}/\text{MeCN}$ (1:1). AFM images of a fresh solution prepared under these conditions, drop-cast onto mica, displayed the formation of toroidal objects^[26] with average external and internal diameters of around 250 and 150 nm, respectively, and ≈ 7 nm profile height (Figure 6, Figure S10a,b). The cross-sectional diameter,



Scheme 2. Schematic representation of the self-assembly of compound **1** at different conditions to form 3D hollow vesicles or toroids.

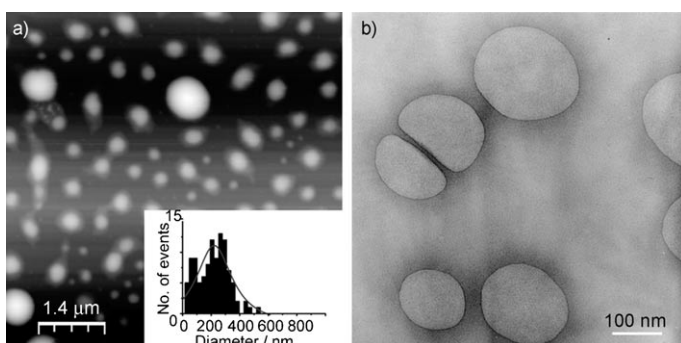


Figure 5. a) Height tapping-mode AFM image (mica, air, 298 K) of **1** in $\text{MeCN}/\text{H}_2\text{O}$ ($\approx 10^{-4}$ M, z scale = 90 nm). The inset in a) corresponds to the mean diameter Lorentzian distribution of the vesicles. b) TEM image, stained with uranyl acetate, of vesicles of **1** from $\approx 10^{-4}$ M, $\text{MeCN}/\text{H}_2\text{O}$ mixtures.

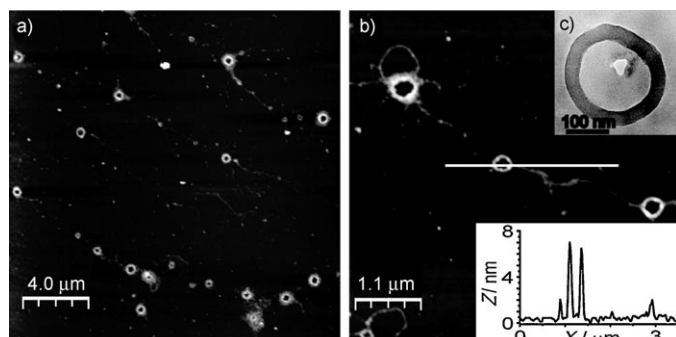


Figure 6. Height tapping-mode AFM images (air, 298 K) of a drop-cast of **1** on mica from freshly prepared $\approx 10^{-6}$ M $\text{MeCN}/\text{H}_2\text{O}$ mixtures [$(z$ scale = 20 nm, for a), and z scale = 12 nm, for b)]. The inset in b) shows the height profile along the line. c) TEM image of **1** from freshly prepared $\approx 10^{-6}$ M $\text{MeCN}/\text{H}_2\text{O}$ mixtures, stained with uranyl acetate.

clearly superior to the gyration radius of **1**, suggests the formation of longitudinal arrays of two molecules of amphiphile **1** that curve to form the toroidal objects. In addition, many of these toroids are interconnected by wires of around 2 nm height (inset in Figure 6b) that could be formed by the π -stacking of **1** into wire-like micelles. The presence of clusters of different morphology could justify the previously mentioned broad distribution of R_H observed in the DLS analysis.

Upon aging this sample for a week, the growing in size and overlapping of the toroids is noticeable (Figure S10c,d).

The toroidal nature of the supramolecular assembly of **1** has been confirmed by TEM imaging (Figure 6c). The inner and outer diameters for the toroids visualized by TEM images are of around 170 and 220 nm, in good correlation with AFM images. These data, together with those extracted from the experiments performed in solution, demonstrate that the presence of water in the self-assembly of **1** is a crucial factor to control the size, as occurs at concentrations of 10^{-4} M, and the morphology of the supramolecular objects. AFM images of a $\approx 10^{-6}$ M solution of **1** in CH₃CN showed micellar hockey puck-like objects with a mean height profile of ≈ 3 nm (Figure S11). This height profile suggests a single molecule coil-rod-coil^[27] aggregation mechanism to form 0D supramolecular ensembles (Scheme S1).

Finally, considering the rotated stacked aggregation suggested by the ¹H NMR experiments carried out in benzene, we have also investigated the morphology of the arrays formed from solutions of **1** in this solvent onto mica. As occurs in DLS measurements, AFM images demonstrate the strong dependence of the morphology on concentration and time. Similarly to our previous triangular radial amphiphile,^[9] freshly prepared or aged $\approx 10^{-6}$ M solutions of **1** in this solvent yield 1D wire-like micelles with average height of ≈ 3.5 nm (Scheme S1, Figure 7a, and Figure S12a). The hydrophilic character of the TEG chains provokes their coiling in this nonpolar solvent and, therefore, a negligible interaction between them, as it is observed in the corresponding concentration-dependent ¹H NMR studies in C₆D₆. The

coiled TEG chains induces compound **1** to rotate through the hydrophobic central core to form wires as a consequence of the joint effect of π - π stacking of molecules of **1** and the positive solvent-solute interactions (Scheme S1).^[9,10]

In sharp contrast, un-uniform micellar clusters with average height of ≈ 7 nm, many of them showing in-plane holes, appear in the AFM images when a more concentrated and freshly prepared ($\approx 10^{-4}$ M) solution of **1** in benzene is utilized (Scheme 1, Figure 7b, and Figure S12b). At this concentration, small columnar stacks of molecules of **1**, intertwined by their TEG chains, could be adsorbed onto the mica surface forming the micellar cluster. After aging the same sample, the rearrangement of these stacks gives rise to the formation of the micellar clusters into a 2D grid-like network with in-plane ellipsoid pores and with a broad height distribution (Figure 7c–e, and Figure S12c).

Conclusions

In summary, we have demonstrated that a simple rectangular amphiphile is readily capable to self-organize to form distinct supramolecular assemblies. The delicate balance of attractive non-covalent forces, mainly solvophobic and π - π stacking interactions between the hydrophobic aromatic part and van der Waals contacts, solvophobic interactions and/or hydrogen bonding between the hydrophilic TEG chains, changes due to the concentration and/or solvent polarity. At $\approx 10^{-4}$ M solutions of **1** in polar solvents, unimolecular curved segments interact to form hollow vesicles whose size increases with increasing polarity. The situation changes drastically at lower concentrations ($\approx 10^{-6}$ M) and only the presence of water in the solvent mixture allows the formation of rather unusual toroids. These results imply that 3D supramolecular architectures of variable morphology could be produced from simple modifications in the external conditions utilized to self-assemble rectangular amphiphiles unlike our previous results from the analogous triangular OPE in which only vesicles are observed in polar solvents.^[9] In addition, the utilization of non polar benzene, favours the apparition of one-dimensional structures that can grow until forming networks, due to the rotated stacking of **1**. The morphology of the arrays formed from this amphiphile onto surfaces is, therefore, directly related with the self-association features observed in solution.

Experimental Section

Amphiphile 1: 1-(2-(2-methoxyethoxy)ethoxy)-4-iodobenzene (**2**) (1.98 g, 5.41 mmol), bis-(triphenylphosphine)-palladium(II)-chloride (0.04 g, 0.06 mmol) and copper (I) iodide (0.01 g, 0.07 mmol) were dissolved in triethylamine (40 mL). The mixture was subjected to several vacuum/argon cycles and 1,2,4,5-tetraethylbenzene (**3b**) (0.21 g, 1.23 mmol) was added. The mixture was heated at 70°C for 2 h and then was allowed to reach room temperature and stirred overnight. After evaporation of the solvent under reduced pressure, the residue was purified by column chromatography (silica gel, CHCl₃/EtOH 99:1) affording

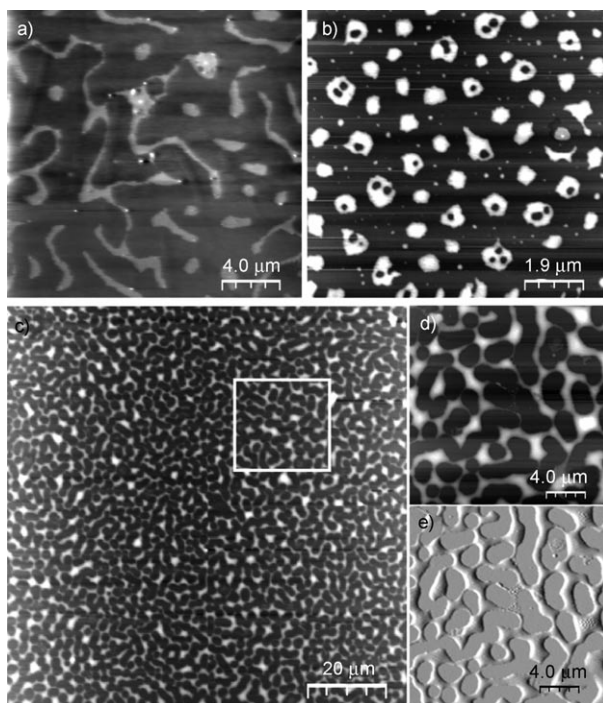


Figure 7. Height tapping-mode AFM images (air, 298 K) of a drop-cast of **1** on mica in benzene: a) $\approx 10^{-6}$ M, (z scale = 13 nm); b) $\approx 10^{-4}$ M, freshly prepared (z scale = 10 nm); c) $\approx 10^{-4}$ M, aged (z scale = 70 nm); d) and e) show the height and phase AFM images of the rectangular area in c) (z scale = 60 nm).

1 as a brown oil (0.82 g, 59%); ^1H NMR (CDCl_3 , 300 MHz) δ = 7.68 (s, 2 H, H_{a}), 7.48 (d, 8 H, H_{b} , J = 8.85 Hz), 6.90 (d, 8 H, H_{c} , J = 8.85 Hz), 4.15 (t, 8 H, H_{d} , J = 6 Hz), 3.87 (t, 8 H, H_{e} , J = 6 Hz), 3.76–3.54 (m, 32 H, $\text{H}_{\text{f+g+h+i}}$); 3.39 ppm (s, 12 H, H_{j}); ^{13}C NMR (CDCl_3 , 75 MHz): δ = 159.5, 134.7, 132.5, 125.4, 115.7, 111.9, 95.7, 85.2, 73.2, 71.9, 71.1, 71.0, 70.0, 67.8, 57.5 ppm; FTIR (neat) $\bar{\nu}$ = 649, 722, 832, 926, 1059, 1108, 1133, 1175, 1199, 1249, 1284, 1352, 1454, 1514, 1568, 1604, 2203, 2873, 2924 cm^{-1} ; MS (MALDI-TOF) m/z : 1126.5; (HRMS): calcd for $\text{C}_{66}\text{H}_{78}\text{O}_{16}$ [M], 1126.53210; found: 1126.52844.

Acknowledgements

We are thankful to Centro de Microscopía y Citometría (UCM) for microscopy imaging; Unidad de Espectroscopía de Infrarrojo-Ramán-Correlación (UCM) for DLS experiments, and Dr. M. Alonso (UAM) for MALDI-TOF spectra. This work has been supported by UCM (UCM-SCH-PR34/07-15826). F.G. and G.F. are indebted to IMDEA-Nanociencia and MEC for a starting research and FPU grants. The authors gratefully acknowledge Prof. N. Martín and his research group.

- [1] a) *Micelles, Membranes, Microemulsions, and Monolayers* (Eds.: W. M. Gelbart, A. Ben-Shaul, D. Roux), Springer, New York, **1994**; b) *Intermolecular and Surface Forces* (Ed.: J. N. Israelachvili), Academic Press, London, **1992**.
- [2] a) S. Jain, F. S. Bates, *Science* **2003**, *300*, 460–464; b) S. Förster, T. Plantenberg, *Angew. Chem.* **2002**, *114*, 712–739; *Angew. Chem. Int. Ed.* **2002**, *41*, 688–714; c) P. Prinsen, P. B. Warren, M. A. J. Michels, *Phys. Rev. Lett.* **2002**, *89*, 148302; d) T. Zemb, M. Dubois, B. Demé, T. Gulik-Krzywicki, *Science* **1999**, *283*, 816–819; e) S. U. Egelhaaf, P. Schurtenberger, *Phys. Rev. Lett.* **1999**, *82*, 2804–2807.
- [3] N. Arai, K. Yasuoka, X. C. Zeng, *J. Am. Chem. Soc.* **2008**, *130*, 7916–7920.
- [4] a) R. M. Capito, H. S. Azevedo, Y. S. Velichko, A. Mata, S. I. Stupp, *Science* **2008**, *319*, 1812–1816; b) F. J. M. Hoeben, I. O. Shklyarevskiy, M. J. Pouderoijen, H. Engelkamp, A. P. H. J. Schenning, P. C. M. Christiaansen, J. C. Maan, E. W. Meijer, *Angew. Chem.* **2006**, *118*, 1254–1258; *Angew. Chem. Int. Ed.* **2006**, *45*, 1232–1236; c) J. P. Hill, W. S. Jin, A. Kosaka, T. Fukushima, H. Ichihara, T. Shimomura, K. Ito, T. Hashizume, N. Ishii, T. Aida, *Science* **2004**, *304*, 1481–1483.
- [5] a) J.-H. Ryu, D.-J. Hong, M. Lee, *Chem. Commun.* **2008**, 1043–1054; b) E. Lee, Y.-H. Jeong, J.-K. Kim, M. Lee, *Macromolecules* **2007**, *40*, 8355–8360.
- [6] a) X. Zhang, Z. Chen, F. Würthner, *J. Am. Chem. Soc.* **2007**, *129*, 4886–4887; b) B.-S. Kim, D.-J. Hong, J. Bae, M. Lee, *J. Am. Chem. Soc.* **2005**, *127*, 16333–16337.
- [7] a) S. Ghosh, X.-Q. Li, V. Stepanenko, F. Würthner, *Chem. Eur. J.* **2008**, *14*, 11343–11357; b) J.-Y. Wang, J. Yan, Z. Li, J.-M. Han, Y. Ma, J. Bian, J. Pei, *Chem. Eur. J.* **2008**, *14*, 7760–7764; c) A. Ajayaghosh, V. K. Praveen, *Acc. Chem. Res.* **2007**, *40*, 644–656; d) A. Ajayaghosh, P. Chithra, R. Varghese, *Angew. Chem.* **2007**, *119*, 234–237; *Angew. Chem. Int. Ed.* **2007**, *46*, 230–233; e) L. Li, H. Jiang, B. W. Messmore, S. R. Bull, S. I. Stupp, *Angew. Chem.* **2007**, *119*, 5977–5980; *Angew. Chem. Int. Ed.* **2007**, *46*, 5873–5876; f) X.-Q. Li, V. Stepanenko, Z. Chen, P. Prins, L. D. A. Siebbeles, F. Würthner, *Chem. Commun.* **2006**, 3871–3873.
- [8] a) W. Cai, G.-T. Wang, Y.-X. Xu, X.-K. Jiang, Z.-T. Li, *J. Am. Chem. Soc.* **2008**, *130*, 6936–6937; b) S. H. Seo, J. Y. Chang, G. N. Tew, *Angew. Chem.* **2006**, *118*, 7688–7692; *Angew. Chem. Int. Ed.* **2006**, *45*, 7526–7530; c) A. Ajayaghosh, R. Varghese, S. Mahesh, V. K. Praveen, *Angew. Chem.* **2006**, *118*, 7893–7896; *Angew. Chem. Int. Ed.* **2006**, *45*, 7729–7732; d) A. Ajayaghosh, R. Varghese, V. K. Praveen, S. Mahesh, *Angew. Chem.* **2006**, *118*, 3339–3342; *Angew. Chem. Int. Ed.* **2006**, *45*, 3261–3264.
- [9] G. Fernández, F. García, L. Sánchez, *Chem. Commun.* **2008**, 6567–6569.
- [10] a) C. A. Hunter, J. K. M. Sanders, *J. Am. Chem. Soc.* **1990**, *112*, 5525–5534; b) C. A. Hunter, K. R. Lawson, J. Perkins, C. J. Urch, *J. Chem. Soc. Perkin Trans. 2* **2001**, 651–669; c) C. H. Hunter, *Angew. Chem.* **2004**, *116*, 5424–5439; *Angew. Chem. Int. Ed.* **2004**, *43*, 5310–5324.
- [11] a) M. Kastler, W. Pisula, D. Wasserfallen, T. Pakula, K. Müllen, *J. Am. Chem. Soc.* **2005**, *127*, 4286–4296; b) T. Q. Nguyen, R. Martel, P. Avouris, M. L. Bushey, L. Brus, C. Nuckolls, *J. Am. Chem. Soc.* **2004**, *126*, 5234–5242; c) J. J. van Gorp, J. Vekemans, E. W. Meijer, *J. Am. Chem. Soc.* **2002**, *124*, 14759–14769; d) F. Würthner, F. Thalacker, A. Sautter, *Adv. Mater.* **1999**, *11*, 754–758.
- [12] a) T. Y. S. But, P. H. Toy, *Chem. Asian J.* **2007**, *2*, 1340–1355; b) S. Dandapani, D. P. Curran, *Chem. Eur. J.* **2004**, *10*, 3130–3138.
- [13] S. Leininger, P. J. Stang, S. Huang, *Organometallics* **1998**, *17*, 3981–3987.
- [14] *Metal-Catalyzed Cross-Coupling Reactions* (Eds.: F. Diederich, P. J. Stang), Wiley-VCH, Weinheim, **1998**.
- [15] *Analytical Methods in Supramolecular Chemistry* (Ed.: C. Schalley), Wiley, New York, **2007**. For recent examples on the utilization of MALDI-TOF to detect supramolecular species interacting by π - π interactions, see: a) G. Fernández, L. Sánchez, E. M. Pérez, N. Martín, *J. Am. Chem. Soc.* **2008**, *130*, 10674–10683; b) G. Fernández, E. M. Pérez, L. Sánchez, N. Martín, *J. Am. Chem. Soc.* **2008**, *130*, 2410–2411; c) C. G. Clark, Jr., R. J. Wenzel, E. V. Andreitchenko, W. Steffen, R. Zenobi, K. Müllen, *J. Am. Chem. Soc.* **2007**, *129*, 3292–3301.
- [16] C. G. Clark, Jr., R. J. Wenzel, E. V. Andreitchenko, W. Steffen, R. Zenobi, K. Müllen, *J. Am. Chem. Soc.* **2007**, *129*, 3292–3301.
- [17] a) E. M. García-Frutos, B. Gómez-Lor, *J. Am. Chem. Soc.* **2008**, *130*, 9173–9177; b) T. V. Jones, M. M. Slutsky, R. Laos, T. F. A. de Greef, G. N. Tew, *J. Am. Chem. Soc.* **2005**, *127*, 17235–17240.
- [18] Oxyethylene chains participate actively in obtaining supramolecular objects. For recent examples, see: a) T. F. A. de Greef, M. M. L. Nieuwenhuizen, P. J. M. Stals, C. F. C. Fitié, A. R. A. Palmans, R. P. Sijbesma, E. W. Meijer, *Chem. Commun.* **2008**, 4306–4309; b) I. Yoshikawa, J. Sawayama, K. Araki, *Angew. Chem.* **2008**, *120*, 1054–1057; *Angew. Chem. Int. Ed.* **2008**, *47*, 1038–1041; c) E. Obert, M. Bellot, L. Bouteiller, F. Andrioletti, C. Lehen-Ferrenbach, F. Boué, *J. Am. Chem. Soc.* **2007**, *129*, 15601–15605.
- [19] a) I. Yoshikawa, J. Sawayama, K. Araki, *Angew. Chem.* **2008**, *120*, 1054–1057; *Angew. Chem. Int. Ed.* **2008**, *47*, 1038–1041; b) E. Obert, M. Bellot, L. Bouteiller, F. Andrioletti, C. Lehen-Ferrenbach, F. Boué, *J. Am. Chem. Soc.* **2007**, *129*, 15601–15605.
- [20] a) R. B. Martin, *Chem. Rev.* **1996**, *96*, 3043–3064; b) D. Zhao, J. S. Moore, *Org. Biomol. Chem.* **2003**, *1*, 3471–3491; c) Z. Chen, A. Lohr, C. R. Saha-Möller, F. Würthner, *Chem. Soc. Rev.* **2009**, *38*, 564–584.
- [21] F. Würthner, C. Thalacker, S. Diele, C. Tschierske, *Chem. Eur. J.* **2001**, *7*, 2245–2253.
- [22] The calculated values for a_n and N by applying the isodesmic model match with previous results obtained for other organic systems capable to self-assemble by π - π stacking aromatic interactions. For recent examples, see: a) Z. Chen, V. Stepanenko, V. Dehm, P. Prins, L. D. A. Siebbeles, J. Seibt, P. Marquetand, V. Engel, F. Würthner, *Chem. Eur. J.* **2007**, *13*, 436–449; b) Reference [21].
- [23] The linear correlation of the inverse of time versus the square of the scattering vector $\langle q \rangle$ obeys the Stokes-Einstein law and allows the calculation of a diffusion coefficient (D) of $4.9 \times 10^{-8} \text{ cm}^2 \text{s}^{-1}$ (see Figure S7). For a detailed discussion, see: *Dynamic Light Scattering* (Eds.: B. J. Berne, R. Pecora), Wiley, New York, **1976**.
- [24] S. Yagai, S. Mahesh, Y. Kikkawa, K. Unoike, T. Karatsu, A. Kitamura, A. Ajayaghosh, *Angew. Chem.* **2008**, *120*, 4769–4772; A. Kitamura, A. Ajayaghosh, *Angew. Chem.* **2008**, *120*, 4769–4772; *Angew. Chem. Int. Ed.* **2008**, *47*, 4691–4694.
- [25] The dimensions of the objects have been determined by subtracting the corresponding tip broadening factors and considering the radius tip (Veeco probes, MPP-11100-10) as 12.5 nm. For the case of the vesicles observed in the AFM images of 10^{-4} M solutions of **1** in MeCN and MeCN/H₂O, the calculated tip broadening factors are

- 10±1 and 26±3 nm, respectively; a) H.-J. Butt, R. Guckenberger, J. P. Rabe, *Ultramicroscopy* **1992**, *46*, 375–393; b) P. Samorí, V. Francke, T. Mangel, K. Müllen, J. P. Rabe, *Opt. Mater.* **1998**, *9*, 390–393.
- [26] For selected examples on toroidal objects, see: a) Z. Nie, D. Fava, E. Kumacheva, S. Zou, G. C. Walker, M. Rubinstain, *Nat. Mater.* **2007**, *6*, 609–614; b) J. C. T. Carlson, S. S. Jena, M. Flenniken, T. Chou, R. A. Siegel, C. R. Wagner, *J. Am. Chem. Soc.* **2006**, *128*, 7630–7638; c) W.-Y. Yang, J. H. Ahn, Y.-S. Yoo, N. K. Oh, M. Lee, *Nat. Mater.* **2005**, *4*, 399–402; d) D. J. Pochan, Z. Chen, H. Cui, K. Hales, K. Qi, K. L. Wooley, *Science* **2004**, *306*, 94–97.
- [27] J.-H. Ryu, M. Lee, *J. Am. Chem. Soc.* **2005**, *127*, 14170–14171.

Received: February 4, 2009

Published online: June 4, 2009